EPJ Web of Conferences **129**, 00019 (2016) DOI: 10.1051/epjconf/201612900019
QCD@Work 2016

Overview of LHCb results on beauty and charm spectroscopy

Antimo Palano[1,⋆]

[1] *INFN and University of Bari, Italy,*
on behalf of the LHCb Collaboration

Abstract. We present a summary of new experimental results from LHCb experiment on the status of the charm spectroscopy using inclusive approaches and Dalitz plot analyses of B and B_s decays. We also summarize latest results on the spectroscopy of heavy baryons.

1 Introduction

The LHCb experiment [1] is collecting very large samples of $c\bar{c}$ and $b\bar{b}$ events. The present results are mostly based on data data collected in 2011 and 2012 during the Run 1 period, corresponding to an integrated luminosity of ≈ 3.0 fb^{-1}.

2 Charm meson spectroscopy

Two methods are used for studying or discovering new states in LHCb.

- Inclusive approach: the study of inclusive final states $D^0\pi^+$, $D^+\pi^-$ and $D^{*+}\pi^-$ in the reactions

$$pp \to D_J X,$$

  and of the final states D^0K^+, $D^+K_s^0$ and $D^{*+}K_s^0$ in the reactions

$$pp \to D_{sJ} X.$$

  In these reactions,

  – All resonances can be produced.
  – The signal to background ratio can be poor.
  – A spin-parity analysis of three-body decays can only distinguish between Natural and Unnatural Parity assignments.
  – No spin analysis is possible for two-body decays.

- Exclusive approach: Dalitz plot analysis of B and B_s decays. In these cases,

  – A full spin-parity analysis is possible.
  – High mass resonances can have low rates or may not be produced.
  – The analysis can be complicated by the presence of multiple interfering contributions.

⋆e-mail: antimo.palano@ba.infn.it

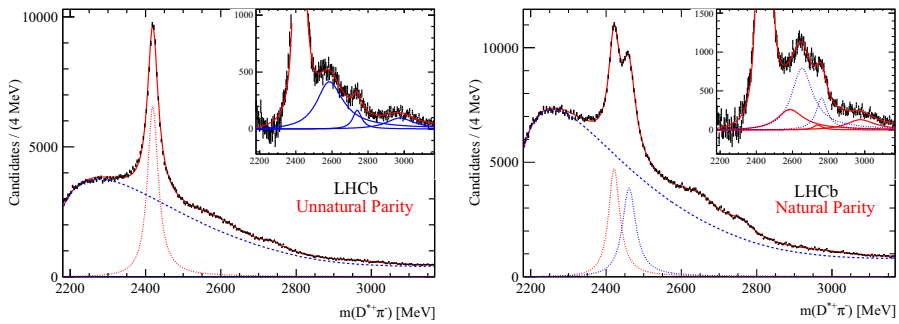

Figure 1. $D^{*+}\pi^-$ mass spectrum with (Left) "Enhanced Unnatural Parity" selections, (Right): "Natural Parity" selections.

2.1 Observation of new D_J mesons

The LHCb experiment has performed an inclusive study of the $D\pi$ and $D^*\pi$ systems using 1 fb^{-1} of data [2]. In the study of the $D^{*+}\pi^-$ system, with $D^{*+} \to D^0\pi^+$, the data are separated in terms of the π^+ helicity angle θ_H . The sample with $|\cos\theta_H| > 0.75$ is defined as "Enhanced Unnatural Parity Sample", while the sample with $|\cos\theta_H| < 0.5$ is defined as "Natural Parity Sample". The two mass spectra are shown in Fig. 1. In the Enhanced Unnatural Parity sample, above the $D_1(2420)$ and $D_2^*(2460)$, three new structures are observed: $D_J(2550)^0$, $D_J(2760)^0$ and $D_J(3000)^0$. In the Natural Parity sample, two further structures are observed: $D_J^*(2600)^0$ and $D_J^*(2760)^0$. The presence of these two Natural Parity states is confirmed by the analysis of the $D^+\pi^-$ and $D^0\pi^+$ data.

2.2 First observation and Dalitz plot analysis of $B^- \to D^+K^-\pi^-$

The $D^+K^-\pi^-$ mass spectrum [3] is shown in Fig. 2 (Left) and contains ≈2000 events in the B^- signal region. A standard Dalitz plot analysis of the $B^- \to D^+K^-\pi^-$ system has been performed. The

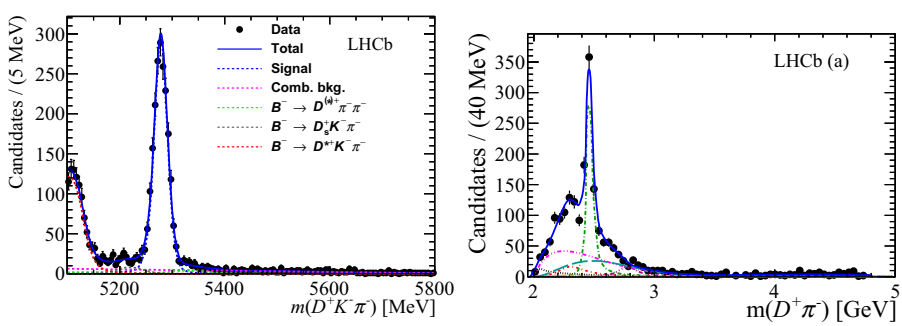

Figure 2. (Left): $D^+K^-\pi^-$ mass spectrum. (Right): $D^+\pi^-$ fit projection with fit result.

best fit is obtained introducing virtual $D_v^*(2007)^0$, B_v^{*0} and nonresonant contributions. A clear spin-2 $D_2^*(2460)$ signal and a $D_J^*(2760)^0$ spin-1 resonance are also observed. The $D^+\pi^-$ fit projection with fit result is shown in Fig. 2(Right). No evidence for a $D_3^*(2760)$ spin-3 resonance is found in this final state.

2.3 Dalitz plot analysis of $B^0 \to \bar{D}^0\pi^+\pi^-$

The $B^0 \to \bar{D}^0\pi^+\pi^-$ [4] signal contains ≈9600 events with 97.8% purity. The $B^0 \to \bar{D}^0\pi^+\pi^-$ Dalitz plot is shown in Fig. 3 (Left). The spin-2 $D_2^*(2460)$ signal along the $\bar{D}^0\pi^-$ axis and the spin-1 $\rho(770)$ signal

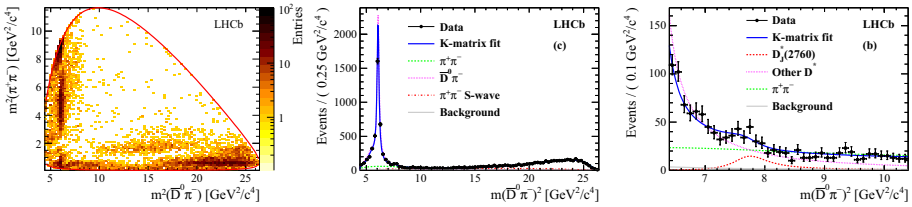

Figure 3. (Left): $B^0 \to \bar{D}^0\pi^+\pi^-$ Dalitz plot. (Center), (Right) $m^2(\bar{D}^0\pi^-)$ fit projection with two different binnings.

along the $\pi^+\pi^-$ axis are observed. The Dalitz plot analysis has been performed using the isobar model and a K-matrix description of the $\pi^+\pi^-$ S-wave. Both methods give a good description of the data. The $m^2(\bar{D}^0\pi^-)$ fit projection is shown in Fig. 3 (Center),(Right). The decay is dominated, in the $\pi^+\pi^-$ system, by S-wave $(16.51 \pm 0.70 \pm 1.68 \pm 1.10)\%$ and $\rho(770)$ $(36.15 \pm 1.00 \pm 2.13 \pm 0.79)\%$. In the $D^0\pi^-$ system, the largest contribution comes from the $D_2^*(2460)^-$ resonance $(28.13 \pm 0.72 \pm 1.06 \pm 0.54)\%$.

The Dalitz plot analysis requires the presence of an additional $J^P = 3^-$ resonance with a K-matrix model fitted fraction of $(1.58 \pm 0.22 \pm 0.18 \pm 0.07)\%$.

2.4 Dalitz plot analysis of $B^0 \to \bar{D}^0K^+\pi^-$

The $B^0 \to \bar{D}^0K^+\pi^-$ [5] signal region contains ≈2300 events. The B^0 Dalitz plot is shown in Fig. 4(Left). The fit projections are shown in Fig. 4(Center),(Right). The decay is dominated by in-

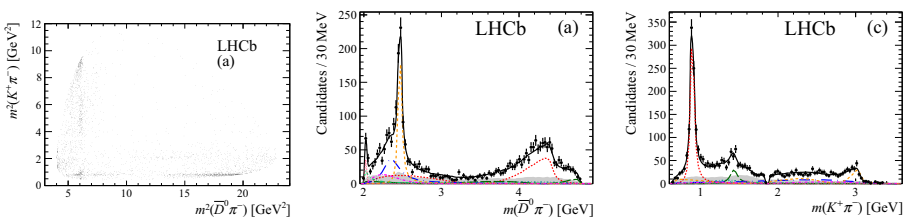

Figure 4. (Left): $B^0 \to \bar{D}^0K^+\pi^-$ Dalitz plot. (Center): $m(\bar{D}^0\pi^-)$ and (Right): $m(K^+\pi^-)$ fit projections.

termediate resonance production of $K^*(892)^0$ $(37.4 \pm 1.5)\%$, $D_0^*(2400)^-$ $(19.3 \pm 2.8)\%$ and $D_2^*(2460)^-$ $(23.1 \pm 1.2)\%$. These Dalitz analyses obtain new parameters for the broad $D_0^*(2400)$ resonance which are summarized in Table 1. No evidence is found for additional spin-1 or spin-3 D_J^* resonances.

3 Results on D_{sJ} mesons spectroscopy

3.1 Dalitz plot analysis of $B_s^0 \to \bar{D}^0K^-\pi^+$

Figure 5(Left) shows the $\bar{D}^0K^-\pi^+$ mass spectrum [8]. The B_s^0 signal contains ≈11000 signal events. The Dalitz analysis shows that the largest components are: $\bar{K}^*(892)^0$ (28.6 %), $D_{s2}^*(2573)^-$ (25.7 %),

Table 1. $D_0^*(2400)$ resonances parameters from the different Dalitz analyses.

Final state	Method	Mass (MeV)	Width (MeV)
$B^0 \to D^0 K^+ \pi^-$	Free	2360 ± 15	255 ± 26
$B^0 \to \bar{D}^0 \pi^+ \pi^-$	Free	2354 ± 7	230 ± 15
$B^- \to D^+ K^- \pi^-$	(PDG)	2318 ± 29	267 ± 40

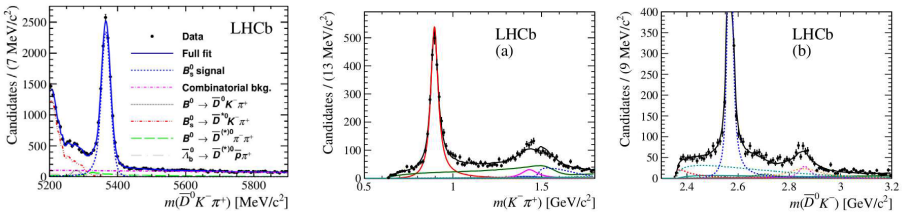

Figure 5. (Left) $\bar{D}^0 K^- \pi^+$ mass spectrum. (Right) $K^- \pi^+$) and $\bar{D}^0 K^-$ mass projections.

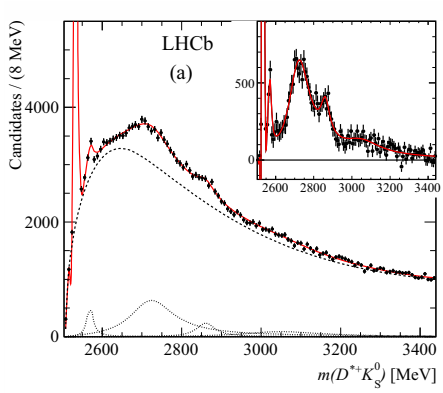

Figure 6. $D^{*+} K_S^0$ with enhanced Natural Parity mass spectrum.

$K\pi$ S-wave (LASS) (21.4 %) $\bar{D}^0 K^-$ nonresonant (12.4 %). A signal present in the 2860 MeV $\bar{D}^0 K^-$ mass region which is described by a superposition of a new spin-1 $(5.0 \pm 1.2 \pm 0.7 \pm 3.3)$ % and a spin-3 $(2.2 \pm 0.1 \pm 0.3 \pm 0.4)$ % resonances. The fitted resonances parameters are:

$m(D_{s1}^*(2860)^-) = 2859 \pm 12 \pm 6 \pm 23$ MeV, $\Gamma(D_{s1}^*(2860)^-) = 159 \pm 23 \pm 27 \pm 72$ MeV,
$m(D_{s3}^*(2860)^-) = 2860.5 \pm 2.6 \pm 2.5 \pm 6.0$ MeV, $\Gamma(D_{s3}^*(2860)^-) = 53 \pm 7 \pm 4 \pm 6$ MeV.

3.2 Inclusive studies

Using samples of 0.36×10^6 $D^+ K_S^0$ and 3.15×10^6 $D^0 K^+$ inclusive candidates [6], the $D_{s1}^*(2710)^+$ and $D_{sJ}^*(2860)^+$ have been observed with parameters consistent with previous measurements [7].

The inclusive $D^{*+} K_S^0$ mass spectrum with enhanced Natural Parity selection is shown in Fig. 6 [9]. Resonances $D_{s1}^*(2710)^+$ and $D_{sJ}^*(2860)^+$ are observed with parameters consistent with those from

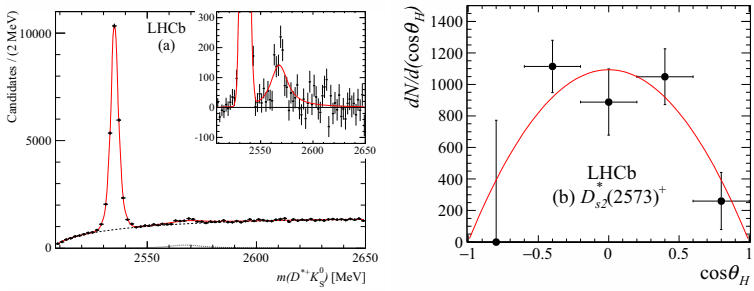

Figure 7. (Left) $D^{*+}K_S^0$ mass spectrum in the threshold region with enhanced Natural Parity selection, (Right) Angular distribution of the $D_{s2}^*(2573)^+ \to D^{*+}K_S^0$.

inclusive and exclusive analyses. Significances are 7.6σ and 7.1σ respectively. A search has been performed for the new spin-1 resonance $D_{s1}^*(2860)^+$ observed in the B_s decay. However, the same χ^2/ndf is obtained in fit that excludes it and its resulting statistical significance is 3.3σ. It is concluded that the data are not sensitive to the presence of the $D_{s1}^*(2860)^+$ resonance.

Figure 7 (Left) shows the threshold region of the $D^{*+}K_S^0$ mass spectrum with enhanced Natural Parity selection. Signals of $D_{s1}(2536)^+$ and $D_{s2}^*(2573)^+$ are observed. $D_{s2}^*(2573)^+$ is observed here for the first time and has a significance of 6.9σ. Its mass is found to be consistent with that obtained from the DK measurements. The $D_{s2}^*(2573)^+$ angular distribution is shown in Fig. 7 (Right) and is consistent with a $J^P = 2^+$ Natural Parity assignment. The relative branching fraction of the decay $D_{s2}^*(2573)^+ \to D^{*+}K_S^0$ is measured as

$$\frac{\mathcal{B}(D_{s2}^*(2573)^+ \to D^{*+}K_S^0)}{\mathcal{B}(D_{s2}^*(2573)^+ \to D^+K_S^0)} = 0.044 \pm 0.005\,(\text{stat}) \pm 0.011\,(\text{syst}). \tag{1}$$

and is in agreement with expectations from quark model calculations which predict a value of 0.058 for this ratio [10].

4 Search for new B^{**} states

The search for new B^{**} states is based on 3 fb^{-1} of data [11]. High purity B^+ (2.5×10^6) and B^0 (1.2×10^6) samples are selected through:

$$B^- \to J/\psi K^-,\ B^{-,0} \to D^{0,-}\pi^+(\pi^+\pi^-)\ [with\ D^0 \to K^-\pi^+(\pi^-\pi^+)],\ B^0 \to J/\psi K^*(892)^0.$$

Figure 8 shows the δm distributions for $B^+\pi^-$ and $B^0\pi^+$ systems. The narrow states are identified as $B_1(5721)^{0,+}$ and $B_2^*(5747)^{0,+}$. New broad states are observed and labelled as $B_J(5840)$ and $B_J(5960)$.

5 New results on baryon spectroscopy

5.1 Observation of excited Λ_b^0 states

The quark model predicts orbitally excited Λ_b^{*0} with $J^P = \frac{1}{2}^+$ and $J^P = \frac{3}{2}^+$ decaying to $\Lambda_b^0\pi^+\pi^-$ or $\Lambda_b^0\gamma$. A clean sample of 70.500 $\Lambda_b \to \Lambda_c\pi^-$ decays in 1.0 fb^{-1} of data is reconstructed, with $\Lambda_c \to pK^-\pi^+$. The $\Lambda_b\pi^+\pi^-$ is shown in Fig. 9 [12]. Two narrow states observed with the following parameters

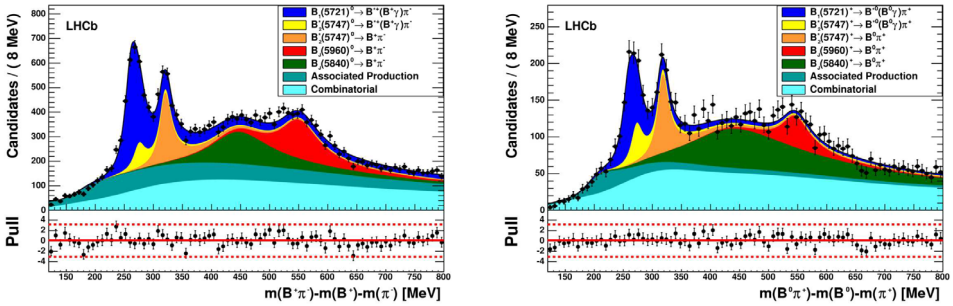

Figure 8. δm distribution for (Left) $B^+\pi^-$ and (Right) $B^0\pi^+$ systems.

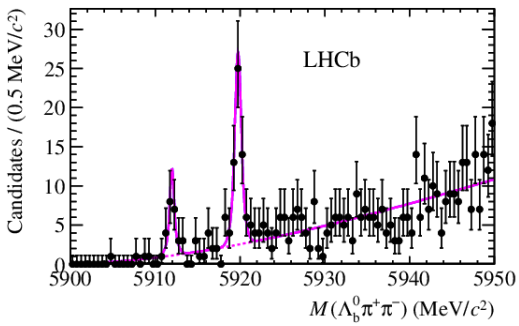

Figure 9. $\Lambda_b\pi^+\pi^-$ mass spectrum.

$M_{\Lambda_b^{*0}(5912)} = 5911.97 \pm 0.12 \pm 0.02 \pm 0.66$ MeV, $\Gamma_{\Lambda_b^{*0}(5912)} < 0.66$ MeV (90% CL),
$M_{\Lambda_b^{*0}(5920)} = 5919.77 \pm 0.08 \pm 0.02 \pm 0.66$ MeV, $\Gamma_{\Lambda_b^{*0}(5920)} < 0.63$ MeV (90% CL).

The $\Lambda_b^{*0}(5912)$ signal contains 17.6 ± 4.8 events and has a significance of 5.2σ; the $\Lambda_b^{*0}(5920)$ signal contains 52.5 ± 8.1 events with a significance of 10.2σ.

5.2 Ξ_b^{*0} Spectroscopy

In 2012, the CMS collaboration [13] observed a new $\Xi_b^{*0} \to \Xi_b^-\pi^+$ state [13]. LHCb has searched for this resonance using $\Xi_b^- \to \Xi_c^0\pi^+$ and $\Xi_c^0 \to pK^-K^-\pi^+$ [14].

Figure 10 shows the $\delta m = m_{cand}(\Xi_b^-\pi^+) - m_{cand}(\Xi_b^-) - m(\pi^+)$ distribution, where a clean $\Xi_b^{*0} \to \Xi_b^-\pi^+$ is observed, confirming the CMS observation.

The resonance parameters are
$m(\Xi_b^{*0}) - m(\Xi_b^-) - m(\pi^+) = 15.727 \pm 0.068 \pm 0.023$ MeV, $\Gamma(\Xi_b^{*0}) = 0.90 \pm 0.16 \pm 0.08$ MeV.
The state is consistent with being the $J^P = 3/2^+$ Ξ_b^{*0} resonance expected in the quark model.

5.3 Observation of two new Ξ_b^- resonances

LHCb experiment has searched for new states in the $\Xi_b^0\pi^-$ mass spectrum, with $\Xi_b^0 \to \Xi_c^+\pi^-$ and $\Xi_c^+ \to pK^-\pi^+$. Figure 11 shows the $\delta m = m_{cand}(\Xi_b^0\pi^-) - m_{cand}(\Xi_b^0) - m(\pi^-)$ distribution where two new states are observed [15].

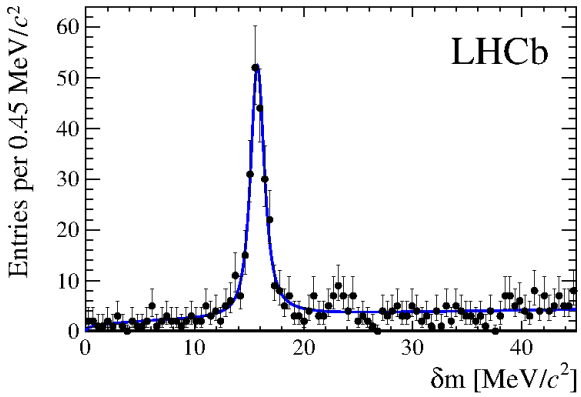

Figure 10. $\delta m = m_{cand}(\Xi_b^-\pi^+) - m_{cand}(\Xi_b^-) - m(\pi^+)$ distribution.

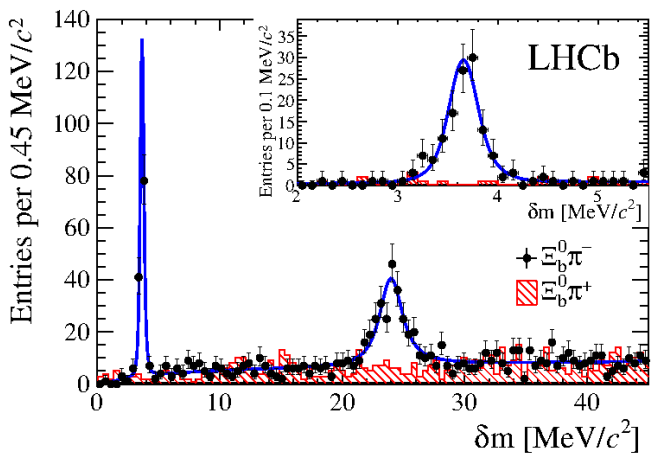

Figure 11. $\delta m = m_{cand}(\Xi_b^0\pi^-) - m_{cand}(\Xi_b^0) - m(\pi^-)$ distribution.

The two states are consistent with being the $J^P = 1/2^+$ $\Xi_b^{\prime -}$ and $J^P = 3/2^+$ Ξ_b^{*-} resonances expected from the quark model in this mass region. Their parameters are measured to be

$m(\Xi_b^{\prime -}) = 5935.02 \pm 0.02 \pm 0.01 \pm 0.50$ MeV, $\Gamma(\Xi_b^{\prime -}) < 0.08$ MeV at 95% C.L.,

$m(\Xi_b^{*-}) = 5955.33 \pm 0.12 \pm 0.06 \pm 0.50$ MeV, $\Gamma(\Xi_b^{*-}) = 1.65 \pm 0.31 \pm 0.10$ MeV.

5.4 Search for Ξ_{cc}^+ states

LHCb experiment has performed an initial search for $\Xi_{cc}^+ \to \Lambda_c K^-\pi^+$ [16] using a small data set (0.65 fb^{-1}). No signal has been found. A more accurate search will be performed using the very high statistics data samples actually available.

6 Summary

- Several new D_J and D_{sJ} mesons have been observed in both inclusive and exclusive B/B_s decays.
- The observation of these states in B/B_s decays allows the determination of their quantum numbers.
- New high statistics data will be shortly available and new decay channels are being analyzed. These studies will allow to better understand the charm and strange-charm spectrum.
- Progress have been performed in completing the quark model spectrum for heavy baryons. Several new states have been discovered. Large progress are expected in the new future in understanding the heavy baryons using high statistics and high purity new decay channels.

References

[1] R. Aaij *et al.* (LHCb Collaboration), Int. J. Mod. Phys. **A30**, 1530022 (2015).
[2] R. Aaij *et al.* (LHCb Collaboration), JHEP **09**, 145 (2013).
[3] R. Aaij *et al.* (LHCb Collaboration), Phys. Rev. **D91**, 092002 (2015).
[4] R. Aaij *et al.* (LHCb Collaboration), Phys. Rev. **D92**, 032002 (2015).
[5] R. Aaij *et al.* (LHCb Collaboration), Phys. Rev. **D92**, 032002 (2015).
[6] R. Aaij *et al.* (LHCb Collaboration), JHEP **10**, 151 (2012).
[7] K.A. Olive *et al.* (Particle Data Group), Chin. Phys. C, **38**, 090001 (2014).
[8] R. Aaij *et al.* (LHCb Collaboration), Phys. Rev. **D90**, 072003 (2014).
[9] R. Aaij *et al.* (LHCb Collaboration), JHEP **02**, 133 (2016).
[10] S. Godfrey and K. Moats, Phys. Rev. **D93**, 034035 (2016).
[11] R. Aaij *et al.* (LHCb Collaboration), JHEP **04**, 024 (2015).
[12] R. Aaij *et al.* (LHCb Collaboration), Phys. Rev. Lett. **109**, 172003 (2012).
[13] S. Chatrchyan *et al.* (CMS Collaboration), Phys. Rev. Lett. **108**, 252002 (2012).
[14] R. Aaij *et al.* (LHCb Collaboration), JHEP **05**, 161 (2016).
[15] R. Aaij *et al.* (LHCb Collaboration), Phys. Rev. Lett. **114**, 062004 (2015).
[16] R. Aaij *et al.* (LHCb Collaboration), JHEP **12**, 090 (2013).